Elastic and Conformational Softness of a Globular Protein

Liang Hong, Dennis C. Glass, Jonathan D. Nickels, Stefania Perticaroli, Zheng Yi, Madhusudan Tyagi, Hugh O'Neill, Qiu Zhang, Alexei P. Sokolov, and Jeremy C. Smith

Phys. Rev. Lett. **110**, 028104 — Published 10 January 2013

DOI: 10.1103/PhysRevLett.110.028104

Elastic and conformational softness of a globular protein

Liang Hong[+,1], Dennis C. Glass[+,1,2], Jonathan D. Nickels[3], Stefania Perticaroli[3], Zheng Yi[1], Tyagi Madhusudan[4], Hugh O'Neill[5,6], Qiu Zhang[5], Alexei P. Sokolov[3] and Jeremy C. Smith[1,6,*]

1. *UT/ORNL Center for Molecular Biophysics, Oak Ridge National Laboratory, P.O.Box 2008, Oak Ridge, TN 37831-6309*
2. *Graduate School of Genome Science and Technology, University of Tennessee, Knoxville, TN 37996-0840*
3. *Joint Institute for Neutron Sciences / Department of Chemistry, Oak Ridge National Laboratory / University of Tennessee, P.O. Box 2008, MS-6453. Bldg. 8630, Suite B201. Oak Ridge, TN 37831*
4. *NIST Center for Neutron Research, 100 Bureau Dr., Gaithersburg MD 20899, and Department of Materials Science and Engineering, University of Maryland, College Park, MD 20742*
5. *Biology and Soft Matter Division, Oak Ridge National Lab, Oak Ridge, TN 37931.*
6. *Department of Biochemistry and Cellular and Molecular Biology, University of Tennessee, Knoxville, TN 37996*

Abstract

Flexibility, or softness, is crucial for protein function, and consists of a "conformational" component, involving jumps between potential wells, and an "elastic" component, involving fluctuations within the wells. Combining molecular dynamics simulation with incoherent neutron scattering and light scattering measurements on green fluorescent protein, we reveal a relationship between the intra-well fluctuations and elastic moduli of the protein. This finding leads to a simple means of experimentally separating the conformational from the elastic atomic displacements.

PACS: 87.15.H-, 87.15.ap, 87.64.Bx, 87.14.E-

[+] Both authors contributed equally

*Author to whom correspondence should be addressed: smithjc@ornl.gov

Protein molecules in their native states, although highly structured, have a degree of flexibility (sometimes called 'softness' [1]) required for their biological function [2, 3]. On short time scales (≤ 1 *ns*) this flexibility has often been characterized by the thermal fluctuations of atomic positions as determined using simulation and scattering techniques [1, 4-7]. These fluctuations are partly conformational, i.e., involving transitions between energy wells [8-10], and partly "elastic", i.e., dynamics confined within single energy wells [9, 10]. The experimental separation of the contributions of these two types of motion to the overall atomic displacements is a fundamental challenge.

The present work addresses this challenge by combining molecular dynamics (MD) simulation with incoherent neutron scattering and light scattering on a globular protein. It is shown that the amplitude of the intra-well motion correlates well with the elastic moduli at *GHz-THz* frequencies. This finding enables a simple and direct method for separating experimentally the conformational from the elastic fluctuations in a protein. Furthermore, insights are obtained into the hydration and temperature dependences of the conformational and elastic protein dynamics.

Incoherent neutron scattering directly probes fluctuations in atomic positions, weighted strongly in favor of hydrogen atoms [1, 4, 5, 11-14]. Here, elastic incoherent neutron scattering experiments were conducted on dry and hydrated green fluorescent protein (GFP) powders using the High Flux Backscattering Spectrometer (HFBS) at the National Institute of Standards and Technology. Experimental details are provided in the Supplemental Material [15]. The intensity of elastic incoherent neutron scattering, *S(q,*

$\Delta t)$, quantifies the atomic motion up to the resolution time of the instrument, Δt, which is ~1 *ns* for HFBS, and is often used to derive the corresponding mean-squared atomic displacement (MSD), $\langle x^2 \rangle$.

The temperature dependence of protein dynamics is key to the present separation of the conformational and elastic components. The experimental $S(q, \Delta t)$ for hydrated and dry GFP measured at different temperatures using HFBS are presented in Fig. 1. The corresponding quantities derived from complementary MD simulations agree quantitatively with experiment over a wide temperature range (detailed simulation protocols and the associated analytical procedures are given in Ref. [15]). Good agreement between the simulation and experiment in $S(q, \Delta t)$ is also apparent for different regions of q (see Fig. S1), further confirming the accuracy of the representation of the *ps-ns* protein dynamics by the MD simulations.

Earlier simulation work showed that protein dynamics on the *ps to ns* time scales can be decomposed into three additive components: localized diffusion, methyl group rotations and non-methyl jumps [10, 16]. The first of these corresponds to atomic fluctuations confined to single energy wells while the other two refer to barrier-crossing events between wells. Typical examples of scatter plots, i.e., projections of single-atom MD trajectories, of these three distinct atomic motions are presented in Figs. 2a, b and c. Here, we apply this decomposition to the MD trajectories of GFP to determine the contributions to the MSD from the three components, denoted as, $\langle x^2 \rangle_{methyl}$, $\langle x^2 \rangle_{jump}$ and $\langle x^2 \rangle_{LD}$, and the results are plotted in Figs. 3a, c and e, respectively.

Over the temperature range 100 - 300 *K*, $\langle x^2 \rangle_{methyl}$, presented in Fig. 3a, is essentially the same in the dry and hydrated GFP, consistent with neutron scattering studies on protein powders demonstrating that the low-temperature (~ 100 to 150 *K*) onset of anharmonicity in the MSD, attributed to activation of the methyl group rotation, is hydration independent [12, 17]. $\langle x^2 \rangle_{methyl}$ is sigmoidal, starting to rise at ~ 100 *K*, and saturating at ~ 270 *K*. This behavior arises from the very similar sigmoidal temperature dependence of the fraction of methyl groups, P_{1ns}, undergoing rotations fast enough to be observed within 1 *ns* (Fig. 3b).

The temperature variation of the non-methyl jumps, $\langle x^2 \rangle_{jump}$, is plotted in Fig. 3c. This variation can, in principle, result from changes of the fraction of atoms that jump (N_{jump}) and/or the jump distance (d_{jump}). Increasing *T* from 100 to 300 *K* raises N_{jump} by orders of magnitude while simultaneously increasing d_{jump} by only 30% (Fig. 3d). Hence, the temperature enhancement of $\langle x^2 \rangle_{jump}$ arises mostly from the thermal activation of the number of jumping states accessible to the protein atoms on the *ns* time scale.

Of particular interest for the present purpose is the MSD resulting from the localized single-well diffusion (Fig. 2a), $\langle x^2 \rangle_{LD}$, displayed in Fig. 3e. As illustrated in Ref. [16], the amplitude of this motion is closely related to the width of the underlying potential of mean force, $W(r) = -k_B T \ln P(r)$, where *P(r)* is the probability distribution of the atomic positions in the corresponding localized-diffusion scatter plot (Fig. 2a) and k_B is the Boltzmann constant. Here, *W(r)* of the localized diffusion of each hydrogen atom was calculated and fitted by a harmonic expression, $\frac{1}{2} k_{LD} r^2$, where k_{LD} is the

associated force constant. The resulting force constant averaged over all hydrogen atoms, $\bar{k}_{LD}$, is plotted versus T in Fig. 3f. At $T > 200\ K$, $\bar{k}_{LD}$ for the hydrated GFP is smaller, i.e., the potential is softer/wider, than for the dry form but the reverse is true at low T, consistent with the differences in $<x^2>_{LD}$ of the two samples in Fig. 3e.

Using a simple harmonic approximation, $< x^2 >_{LD} = C\frac{k_B T}{\bar{k}_{LD}}$, where C is a constant independent of temperature and hydration, and $\bar{k}_{LD}$ is the average force constant estimated from *W(r)* of the localized diffusion, one can reproduce the $<x^2>_{LD}$ in both dry and hydrated GFP over the whole temperature range from 10 to 300 *K* (Fig. 3e). Hence, the temperature and hydration dependences of the localized diffusion are essentially determined by those of $\bar{k}_{LD}$, i.e., the average curvature of the individual energy wells, consistent with the energy wells being effectively harmonic [16].

Light scattering experiments directly probe frequencies associated with elastic modes. Of these, Brillouin modes present at ~ 10 *GHz*, are propagating sound waves with wavelengths of ~ 100 *nm* [18], thus characterizing inter-protein interactions. The frequencies of the Brillouin modes provide a direct estimate of the *GHz* elastic modulus of the protein [18]. This modulus involves equilibrium fluctuations in the native protein state, as distinct from the mechanical properties of unfolding/denaturing proteins measured using, for example, atomic force microscopy [19]. The elastic modulus, M, of a crystal with one atom in the primitive cell is proportional to the interatomic force constant, k, as $M = k/a$, where a is the interatomic distance [20]. Given a typical value of a in proteins of ~ 1.5 Å, the force constants for hydrated and dry GFP at room

temperature in Fig. 3f would correspond to M = 5 and 9 *GPa*, respectively. These values are consistent with the Brillouin light scattering on lysozyme crystals in which, when decreasing the relative humidity from 98% to 67% [18] (corresponding to a change of hydration level from 0.4 to 0.15 gram water / gram protein [21]), the longitudinal modulus at room temperature changes from 5 to 12 *GPa* along the [001] face and from 13 to 22 *GPa* along the [110] face.

Corresponding BLS experiments were performed on both dry and hydrated GFP (see Ref. [15]). The inset of Fig. 3f presents the temperature dependence of the frequency (ν_L) of the longitudinal sound wave, the square of which gives the longitudinal modulus. At T > 200 K, ν_L in hydrated GFP is lower, i.e., the system is softer, than in the dry sample, but the reverse is true when T < 200 K. These data strongly support the analysis of $\bar{k}_{LD}$ in Fig. 3f, and are also consistent both with recent simulation findings that at room temperature surface hydration softens/widens $W(r)$ [16], and with the experimental and simulation result that, below ~ 180 - 190 K, the hydration water becomes glassy, substantially hardening the encapsulated protein molecules [22-24].

In addition to Brillouin modes, the Boson peak of the hydrated GFP was also measured using light scattering (see Ref. [15]). This peak arises from collective vibrations at ~ 1 *THz* distributed over the protein molecule [25, 26], The temperature dependences of the squared frequency of the Brillouin mode (ν_L^2) and the Boson peak (ν_{BP}^2) reflect corresponding variations of the *GHz* and *THz* elastic moduli, respectively. As shown in Figs. 4a and b, ν_L^2 and ν_{BP}^2 exhibit temperature dependences very similar to $\bar{k}_{LD}$, and this was also found to be true for another protein, lysozyme. These two proteins

differ significantly in structure, GFP having a β-barrel structure whereas lysozyme, a two-domain protein linked via a hinge, consists of comparable amounts of helices and β-sheets. This result suggests some generality in the finding that the effective force constant estimated from the potential of mean force of the localized diffusion might be defined by the equilibrium mechanical properties of proteins in the native state, i.e., the *GHz-THz* elastic moduli. As shown in Ref. [16], the localized diffusion of individual protein atoms is highly coupled, presenting as correlated modes running through the entire protein molecule. This collective character is consistent with the connection to the elastic moduli, which are estimated from the collective vibrational modes involving the whole macromolecule, i.e., the Brillouin modes and the Boson peak. $\bar{k}_{LD}$ can thus be considered as an "effective" rigidity or stiffness of the macromolecule, in agreement with the microscopic description of the elastic moduli.

The present findings lead to a means of experimentally separating the conformational and elastic contributions to protein atomic displacements. To do this, the temperature-dependent overall $<x^2>$ is measured using incoherent neutron scattering, and $<x^2>_{LD}$ is approximated as $B\frac{k_B T}{\nu^2}$, where ν is the frequency of either the Brillouin mode or the Boson peak probed via light scattering or neutron scattering, and B is a constant that can be determined by matching $B\frac{k_B T}{\nu^2}$ with $<x^2>$ measured at temperatures ≤ 100 K, temperatures at which barrier-crossing events do not yet occur (Figs. 3a to d). The difference between $<x^2>$ and $<x^2>_{LD}$ at T > 100 K then quantifies the conformational

contribution $<x^2>_{conf}$. An example of such an analysis, performed on hydrated GFP, is given in Fig. 4c.

In Ref. [1], the temperature dependence of the *ns* MSD measured using incoherent neutron scattering was used to characterize the rigidity, i.e., the "resilience", of a protein by defining an effective force constant, $k_{all} = \frac{k_B}{\frac{d<x^2>}{dT}}$ (denoted here as k_{all} to differentiate it from k_{LD}) [1, 4-6]. In the last decade, k_{all} has been widely used to characterize the softness of proteins and its response to external conditions, such as temperature, hydration and solvation. In particular, it was shown that for hydrated proteins k_{all} usually decreases by an order of magnitude when increasing the temperature from ~ 100 *K* to room temperature [1, 4-6]. This large temperature variation is confirmed in the present work (see Figs. 4a and b). However, over the same temperature range, k_{LD}, ν_L^2 and ν_{BP}^2 change only by a factor of ~ 2. This drastic difference results from the fact that k_{all} is estimated from the total $<x^2>$, which, at $T > 100$ *K*, contains both intra-well and barrier-crossing motions (Fig. 3). Barrier crossing varies strongly with temperature as conformational states become accessible on the *ns* time scale (Figs. 3b and d), and this corresponds to thermally-induced conformational flexibility. However, this conformational flexibility is not directly related to the equilibrium mechanical properties of proteins, i.e., k_{LD} or *M*, but rather to the energy barriers and jump distances. For example, methyl group rotation, a typical barrier-crossing event, behaves essentially the same in dry and hydrated proteins (Figs. 3a and b and Ref. [16]) although these two differ significantly in k_{LD} and *M* (Fig. 3f and Ref. [18]). Hence, defining a force constant

through the total atomic displacement, i.e., $\frac{k_B}{\frac{d<x^2>}{dT}}$, confounds conformational and elastic atomic fluctuations.

Incoherent neutron scattering, light scattering and MD simulation have been combined here to demonstrate a direct correlation between the amplitude of intra-well fluctuations and the equilibrium mechanical properties of proteins in the native state. This result suggests that the curvature of the potential of mean force for intra-well atomic motions is determined by the elastic moduli. This discovery provides an experimental means of dissecting the conformational from the elastic contribution to flexibility, which should be of general use in future work on the relationship of protein dynamics to function and to their chemical and 3-D structure.

Acknowledgement

The authors acknowledge financial support from an EPSCOR grant from the U.S. Department of Energy (grant DE-FG02-08ER46528). This work utilized facilities supported in part by the National Science Foundation under Agreement No. DMR-0944772.

Reference

[1] G. Zaccai, Science **288**, 1604 (2000).

[2] K. A. Henzler-Wildman *et al.*, Nature **450**, 7171 (2007).

[3] B. F. Rasmussen *et al.*, Nature **357**, 423 (1992).

[4] D. J. Bicout and G. Zaccai, Biophys. J. **80**, 1115 (2001).

[5] K. Wood *et al.*, Chem. Phys. **345**, 305 (2008).

[6] Z. Yi *et al.*, J. Phys. Chem. B **116**, 5028 (2012).

[7] H. Frauenfelder, G. A. Petsko, and D. Tsernoglou, Nature **280**, 558 (1979).

[8] R. Elber and M. Karplus, Science **235**, 318 (1987).

[9] H. Frauenfelder, S. G. Sligar, and P. G. Wolynes, Science **254**, 1598 (1991).

[10] L. Hong, N. Smolin, B. Lindner, A. P. Sokolov and J. C. Smith, Phys. Rev. Lett. **107**, 148102 (2011).

[11] W. Doster, S. Cusack, and W. Petry, Nature **337**, 754 (1989).

[12] J. H. Roh *et al*., Phys. Rev. Lett. **95**, 038101 (2005).

[13] S. H. Chen *et al.*, Proc. Natl. Acad. Sci. U.S.A. **103**, 9012 (2006).

[14] M. Ferrand *et al.*, Proc. Natl. Acad. Sci. U.S.A. **90**, 9668 (1993).

[15] Supplemental Material.

[16] L. Hong, X. Cheng, D. C. Glass, and J. C. Smith, Phys. Rev. Lett. **108**, 238102 (2012).

[17] G. Schiro *et al.*, Phys. Chem. Chem. Phys. **12**, 10215 (2010).

[18] S. Speziale *et al.*, Biophys. J. **85**, 3202 (2003).

[19] M. Rief *et al.*, Science **276**, 1109 (1997).

[20] C. Kittel, Introduction to Solid State Physics (John Wiley & Sons, Inc, USA, 2005), p. 77 - 92.

[21] J. A. Rupley and G. Careri, Adv. Protein Chem. **41**, 37 (1991).

[22] K. Moritsugu and J. C. Smith, J. Phys. Chem. B **109**, 12182 (2005).

[23] S. Khodadadi, A. Malkovskiy, A. Kisliuk and A. P. Sokolov, Biochim. Biophys. Act. **1804**, 15 (2010).

[24] J. D. Nickels *et al.*, Biophys. J. **103**, 1566 (2012).

[25] M. Tarek and D. J. Tobias, J. Chem. Phys. **115**, 1607 (2001).

[26] G. Caliskan *et al.*, J. Chem. Phys. **121**, 1978 (2004).

Figure Caption

Fig. 1 (color online). Experimental and simulation-derived $S(q, \Delta t)$, normalized by the value at ~ 10 K and averaged over 11 values of q, ranging from 0.62 to 1.68 $Å^{-1}$ for (a) dry (h = 0.05) and (b) hydrated (h = 0.4) GFP. The experimental data are solid symbols whereas the values derived from MD are empty symbols (The same notations are used in all other figures). The error bars of the simulation-derived results are the standard deviations obtained from ten independent MD trajectories performed at each temperature, the same for all other figures.

Fig. 2 (color online). Typical examples of scatter plots of non-exchangeable hydrogen atoms. (a) localized diffusion (single-well motion) (atom HA of residue ALA37); (b) two-site jumps (atom HD1 of residue ARG 73); and (c) methyl group rotation (atom HB1 of residue ALA 37).

Fig. 3 (color online). (a) $\langle x^2 \rangle_{methyl}$. (b) Fraction of methyl groups with rotation relaxation times ≤ 1 *ns*. (c) $\langle x^2 \rangle_{jump}$. (d) Number of jumping atoms. The inset in (d) is the average jump distance. (e) $\langle x^2 \rangle_{LD}$, the symbols represent the values directly derived from the MD trajectories while the solid curves denote harmonic approximations of $C\frac{k_B T}{\bar{k}_{LD}}$. (f) Average force constant $\bar{k}_{LD}$, derived from the MD potential of mean force of the localized

diffusion of protein atoms. The inset of (f) is the frequency of longitudinal sound waves, ν_L, measured using Brillouin light scattering.

Fig. 4 (color online). Temperature dependence of $\bar{k}_{LD}$ (○), k_{all} derived from the experimental $\langle x^2 \rangle$ (■), k_{all} estimated from the simulation-derived $\langle x^2 \rangle$ (□), ν_L^2 (▲) and ν_{BP}^2 (♦) for hydrated (a) GFP and (b) lysozyme, normalized to the values at 100 *K*. The experimental $\langle x^2 \rangle$ of GFP and lysozyme used to derive k_{all} were obtained from Refs. [24] and [12], respectively. k_{all}, defined in the text, was estimated over temperature intervals of 100 *K*, e.g., k_{all} at 300 *K* was calculated over the range 200 - 300 *K*. The light scattering data (ν_L and ν_{BP}) of GFP are obtained in the present work whereas those for lysozyme are from Ref. [23]. (c) Direct experimental separation of the elastic $\langle x^2 \rangle_{LD}$ ($= B\frac{k_B T}{\nu_L^2}$) and the conformational $\langle x^2 \rangle_{conf}$ ($=\langle x^2 \rangle - \langle x^2 \rangle_{LD}$) contributions to $\langle x^2 \rangle$ (Ref. [24]) of hydrated GFP. Constant *B* is determined by matching $B\frac{k_B T}{\nu_L^2}$ with $\langle x^2 \rangle$ at ~ 100 *K*. Error bars throughout the text represent one standard deviation.

Fig. 1

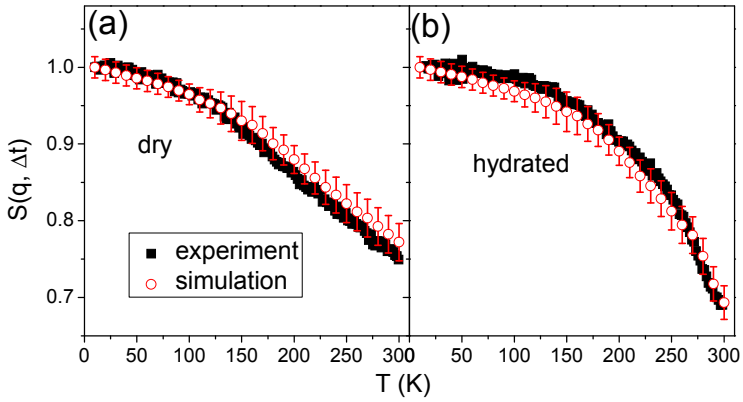
(a)
(b)
dry
hydrated
experiment
simulation
S(q, Δt)
T (K)
1.0
0.9
0.8
0.7
0
50
100
150
200
250
300

Fig. 2

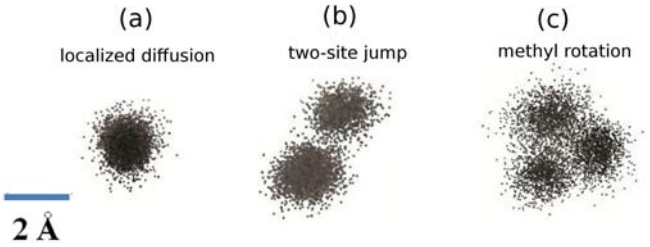

Fig. 3

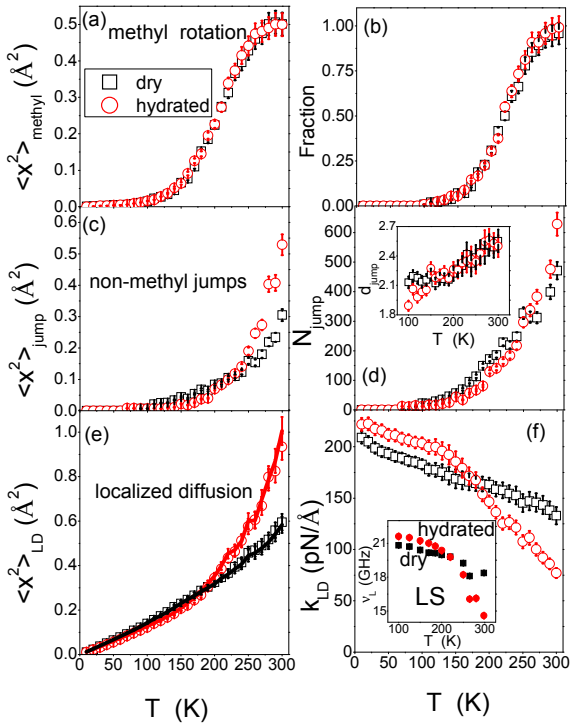
(a) methyl rotation
dry
hydrated
<x²>methyl (Å²)
(b)
Fraction
(c)
non-methyl jumps
<x²>jump (Å²)
Njump
djump
T (K)
(d)
(e)
localized diffusion
<x²>LD (Å²)
(f)
kLD (pN/Å)
hydrated
dry
LS
ν_L (GHz)
T (K)

Fig. 4

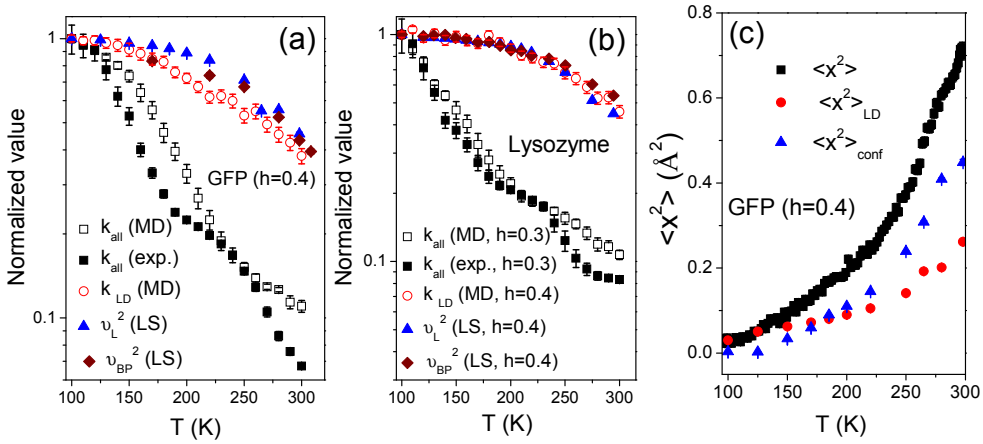
(a)
GFP (h=0.4)
Normalized value
T (K)
k_all (MD)
k_all (exp.)
k_LD (MD)
υ_L^2 (LS)
υ_BP^2 (LS)
(b)
Lysozyme
k_all (MD, h=0.3)
k_all (exp., h=0.3)
k_LD (MD, h=0.4)
υ_L^2 (LS, h=0.4)
υ_BP^2 (LS, h=0.4)
(c)
<x^2>
<x^2>_LD
<x^2>_conf
GFP (h=0.4)
<x^2> (Å^2)